



Napieralski, S. A., Buss, H. L., Brantley, S. L., Lee, S., Xu, H., & Roden, E. E. (2019). Microbial chemolithotrophy mediates oxidative weathering of granitic bedrock. *Proceedings of the National Academy of Sciences of the United States of America*, 116(52), 26394-26401. <https://doi.org/10.1073/pnas.1909970117>

Peer reviewed version

Link to published version (if available):
[10.1073/pnas.1909970117](https://doi.org/10.1073/pnas.1909970117)

[Link to publication record in Explore Bristol Research](#)
PDF-document

University of Bristol - Explore Bristol Research

General rights

This document is made available in accordance with publisher policies. Please cite only the published version using the reference above. Full terms of use are available:
<http://www.bristol.ac.uk/red/research-policy/pure/user-guides/ebr-terms/>



Supplementary Information for

Microbial chemolithotrophy mediates oxidative weathering of granitic bedrock

Stephanie A. Napieralski, Heather L. Buss, Susan L. Brantley, Seungyeol Lee, Huifang Xu and Eric E. Roden

Stephanie A. Napieralski and Eric E. Roden
Email: snapieralski@wisc.edu; eroden@geology.wisc.edu

This PDF file includes:

Figs. S1 to S4
Tables S1 to S2

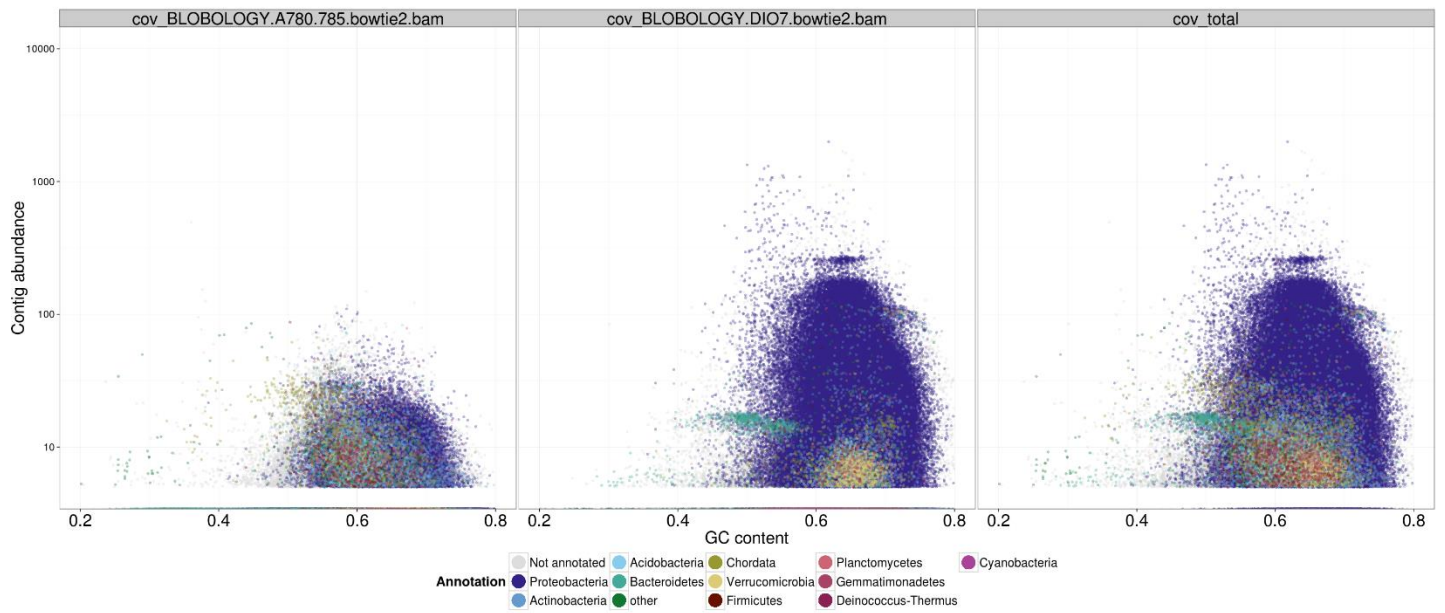


Fig. S1. GC versus contig abundance Blob plots of individual contigs (n= 584329) from the total coassembly (right) and the *in situ* metagenome (left) obtained from 7.85 m depth (Sample A) and a quartz diorite enrichment culture from the same inocula (center), colored by phylum level classification demonstrating a decrease in community complexity and enrichment in *Betaproteobacteria* in the enrichment culture.

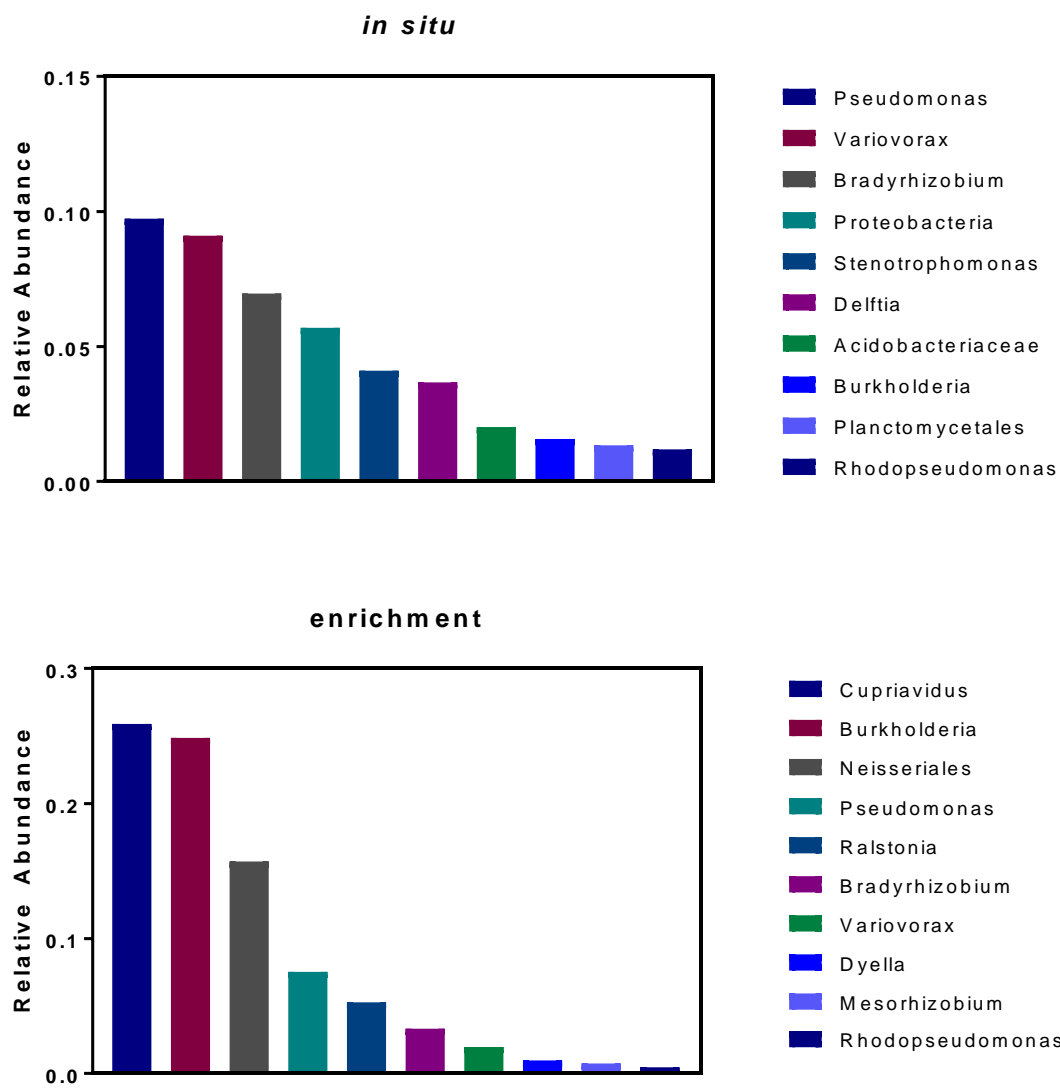
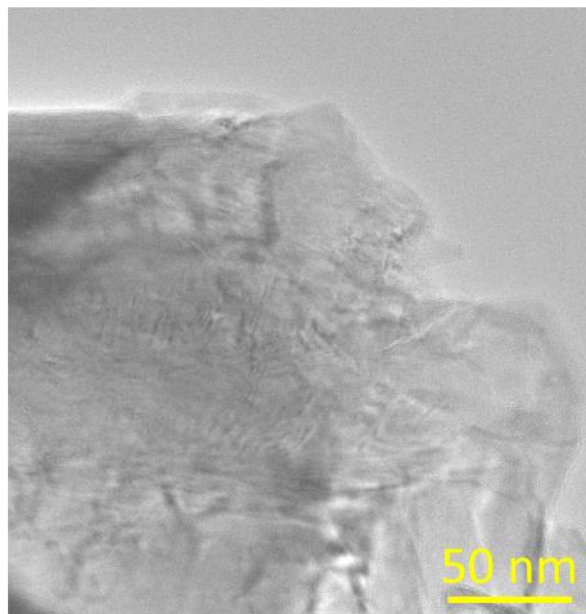
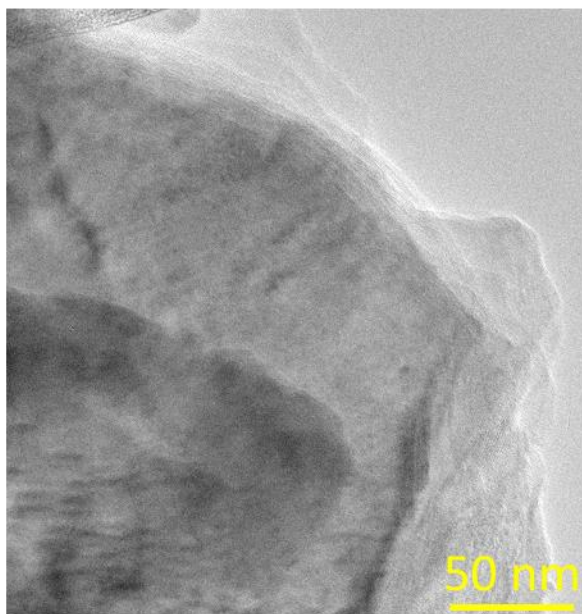


Fig. S2. Relative abundance of the 10 most abundant genera, or higher taxonomic classification if unable to achieve genera-level classification in the *in situ* (top) and enrichment culture (bottom) metagenomes based on taxonomic classification of individual reads.

Unoxidized control biotite



Microbially oxidized biotite

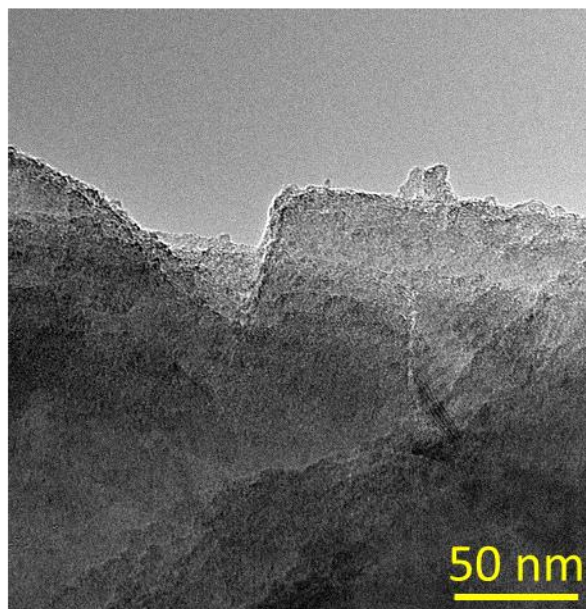
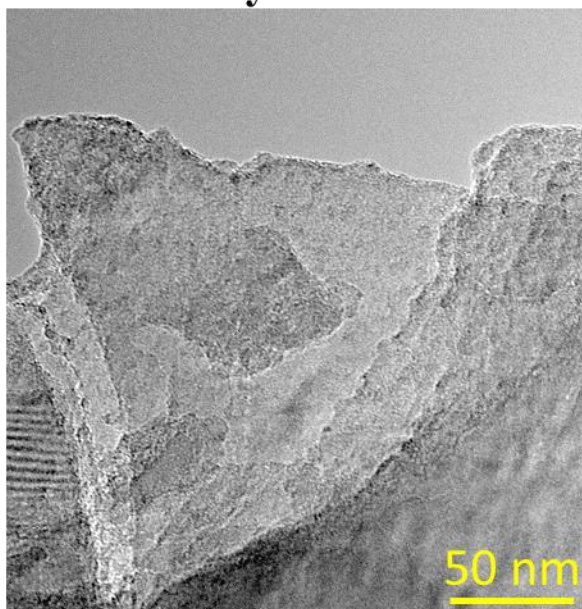
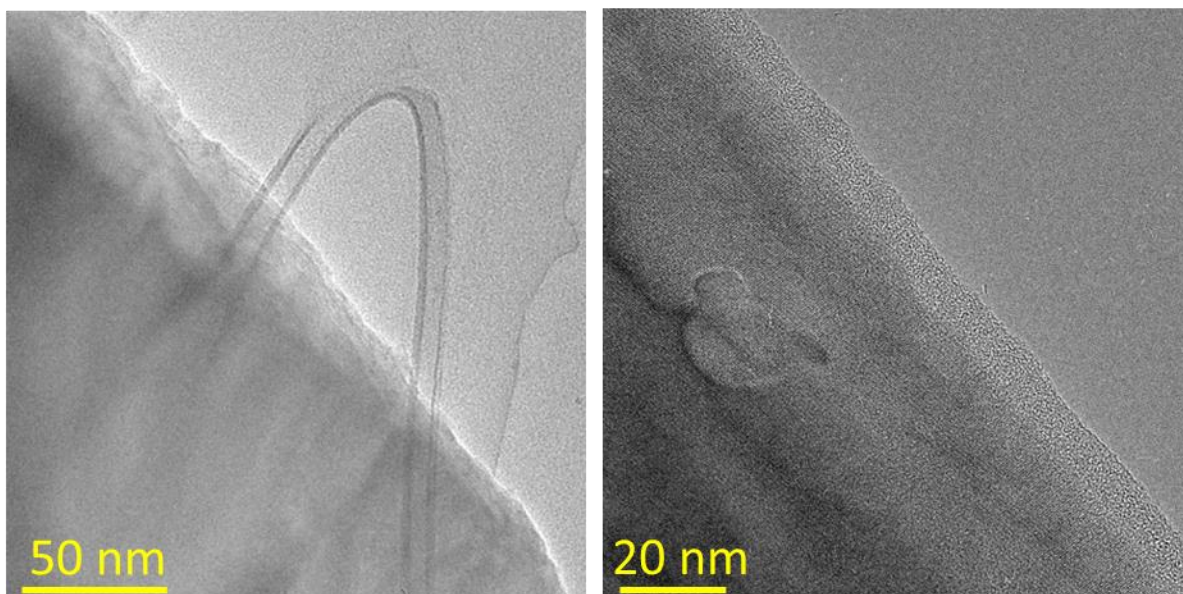


Fig. S3. Bright field TEM images comparing abiotic control (top) and microbially oxidized (bottom) biotite surfaces after 864 days incubation.

Unoxidized control hornblende



Microbially oxidized hornblende

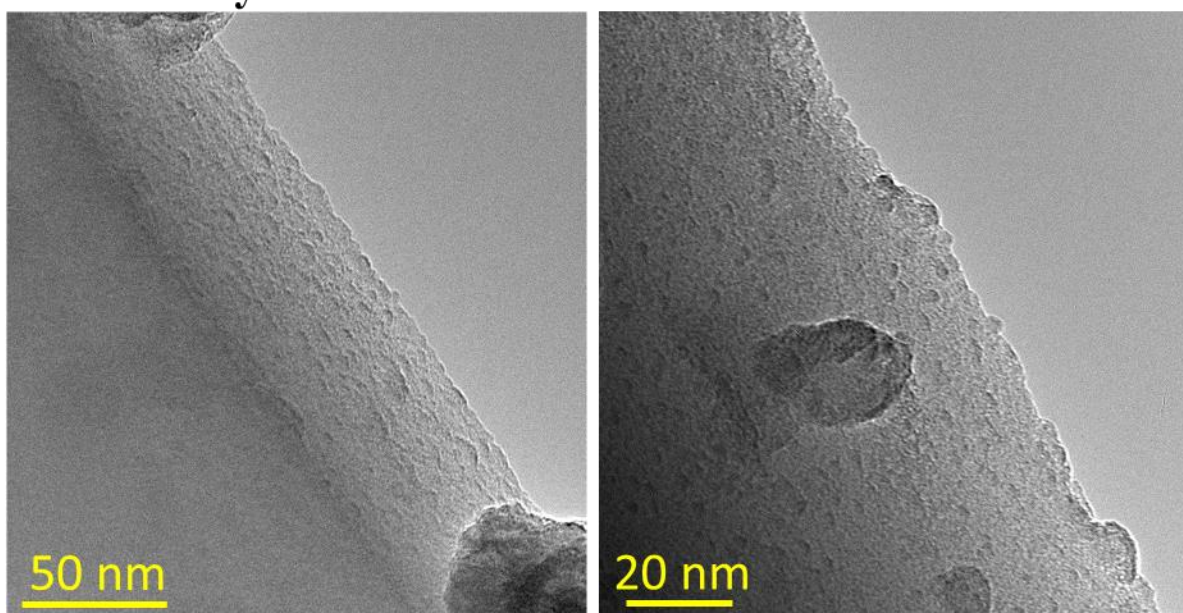


Fig. S4. Bright field TEM images comparing abiotic control (top) and microbially oxidized (bottom) hornblende surfaces after 864 days of incubation.

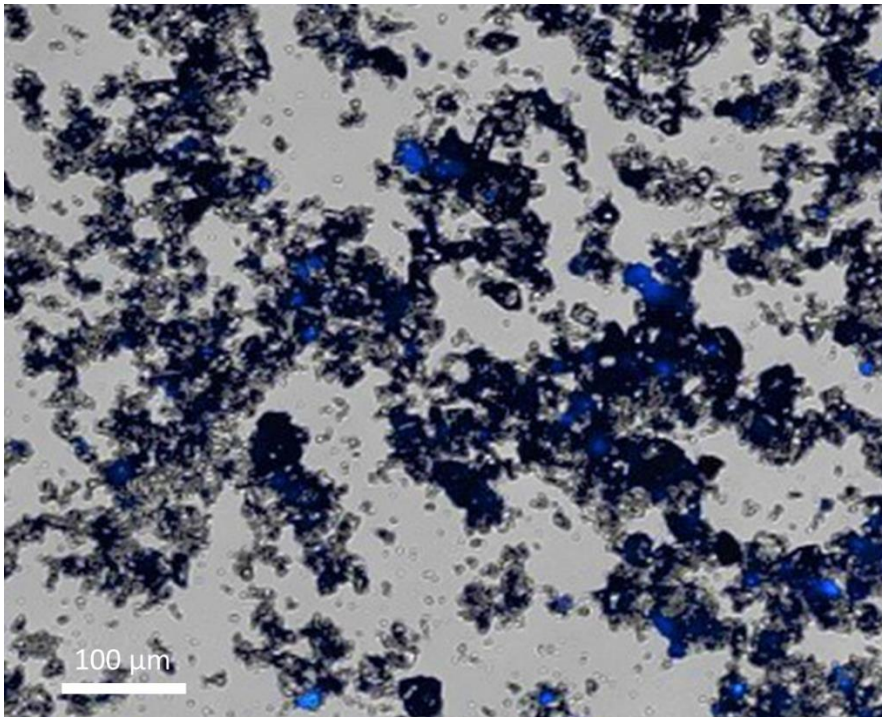


Fig. S5. Composite image (epifluorescence and light) of DAPI stained diorite oxidizing enrichment culture showing close association of cells (bright blue spots) with mineral grains.

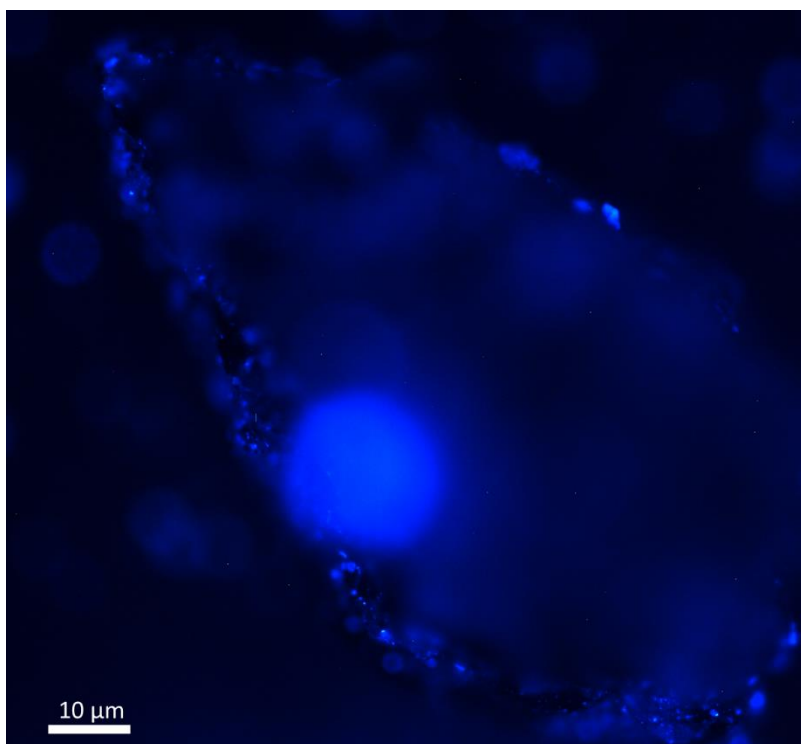


Fig. S6. Epifluorescence microscopy of a DAPI stained individual biotite grain obtained from enrichment culture revealing sparse microbial colonization of mineral edges.

Table S1 Calculated growth yields in $\mu\text{mol biomass C } \mu\text{mol}^{-1} \text{ Fe(II)}$ oxidized in individual reactors.

Sample	nM ATP	g C/L	$\mu\text{mol C/mL}$	Initial Fe(II) $\mu\text{mol/mL}$	Initial Fe(II)/Fe(tot)	Final Fe(II)/Fe(tot)	Δ Fe(II)/Fe(tot)	Fe(II) oxidized	yield
A1	1.646	0.00016	0.014	7.442	0.697	0.572	0.125	0.930	0.015
A2	1.751	0.00018	0.015	7.161	0.674	0.572	0.102	0.730	0.020
B1	3.142	0.00031	0.026	7.174	0.728	0.535	0.193	1.385	0.019
B2	2.045	0.00020	0.017	7.711	0.763	0.593	0.170	1.311	0.013
C1	3.033	0.00030	0.025	8.430	0.787	0.787	0.000	0.000	n/a
C2	3.007	0.00030	0.025	7.665	0.755	0.674	0.081	0.621	0.040

Table S2 Abundance of major elements in the Rio Blanco Quartz Diorite as determined by aqua regia digestion and ICP-OES analysis.

Element	Abundance (wt %)
Al	7.17
Ca	3.87
Fe	3.81
K	1.06
Mg	1.33
Na	2.04
Ti	0.304